To be published in the Proceedings of the NATO A.S.I. on "High Temperature Superconductors", Bad Windsheim (FRG), 13-26 August 1989.

OXYGEN EVOLUTION IN HIGH Tc SUPERCONDUCTORS

B. WUYTS, J. VANACKEN, J.-P. LOCQUET(°), C. VAN HAESENDONCK, IVAN K. SCHULLER* and Y. BRUYNSERAEDE
Laboratorium voor Vaste Stof-Fysika en Magnetisme, Katholieke Universiteit Leuven, B-3030 Leuven, Belgium; * Physics Department - B019, University of California - San Diego, La Jolla, California 92093, USA; (°) Present address : IBM Research Division, Zürich Research Laboratory, 8803 Rüschlikon, Switzerland.

ABSTRACT. We have performed extensive gas evolution and superconducting measurements on a series of high temperature ceramics as a function of oxygen and metal ion composition. In $YBa_2Cu_3O_{7-\delta}$, the oxygen evolution kinetics at fixed temperature (400°C) and vacuum ($P \simeq 10^{-6}$ Torr) for varying lengths of time, is found to proceed by an initial large change in "chain" occupancy and a subsequent leveling off. The critical temperature obtained from susceptibility measurements drops from 90 K to 60 K as the oxygen content in the "chains" decreases. Longer annealing yields a decrease of the 60 K superconducting fraction, probably due to oxygen disorder effects since the total oxygen content stays constant.

1 Introduction

Much evidence has been presented for the dependence of superconductivity on oxygen content in high temperature superconductors, especially in $YBa_2Cu_3O_{7-\delta}$ (YBCO) and related compounds [1]. Nevertheless, a complete comprehensive picture relating the oxygen content and ordering to the superconducting properties has not yet emerged. Moreover, sample preparation methods, including details of oxygen doping, can often lead to large differences in physical properties.

Since the discovery of the ceramic high T_c materials, we have studied the oxygen kinetics using combined gas evolution, diffraction, transport and magnetic measuring techniques. In this way, it is possible to establish the relative amounts of oxygen present in the oxide at various preparation and annealing stages. Secondly, by using a single site desorption relation it is possible to extract from the evolution curves interesting thermodynamic parameters such as the activation energies and escape frequencies for the different oxygen sites. Moreover, these types of measurements can give information on oxygen thermodynamics for bulk samples as well as for thin films. In conjunction with structural and physical properties, we hope to obtain a complete description of the relationship between oxygen stiochiometry, ordering and superconductivity.

Here, we present a detailed study of changes in oxygen stoichiometry and superconductivity after long annealing times at 400°C. As shown earlier [2], the critical temperature (defined as the midpoint of the transition) drops from 90 K to 60

K, following the changes in oxygen occupancy of the Cu-O chain sites. However, changes in the width of the superconducting transition indicate the presence of inhomogeneities for most annealing times. Interestingly, these changes in transition width occur even at constant oxygen stoichiometry, indicating the possible importance of oxygen ordering for superconductivity. Gas evolution studies on Pr doped YBCO have been performed in order to clarify the origin of the superconductivity in this system. Moreover, studies on MBE prepared thin films show gas evolution to be a powerful technique for studies where the small amounts of material present do not permit the application of classical techniques such as thermogravimetry.

2 Experimental Techniques

2.1 Oxygen Evolution Technique

One of the most commonly used techniques to measure the oxygen content in high T_c oxides is thermogravimetric analysis (TGA) where the weight change of a sample is recorded as a function of temperature. Although this technique accurately determines the oxygen content in large bulk samples [3], it does not provide microscopic information such as binding energies and is not applicable for thin films. The gas evolution technique presented here is complementary to TGA. It determines the amount of gas evolved from the sample as a function of temperature [1,4,5]. Moreover, this technique,when combined with mass spectrometry, allows an accurate compositional analysis of the evolved gases and can also be applied in situations where inherently only small amounts of material are available such as for thin films.

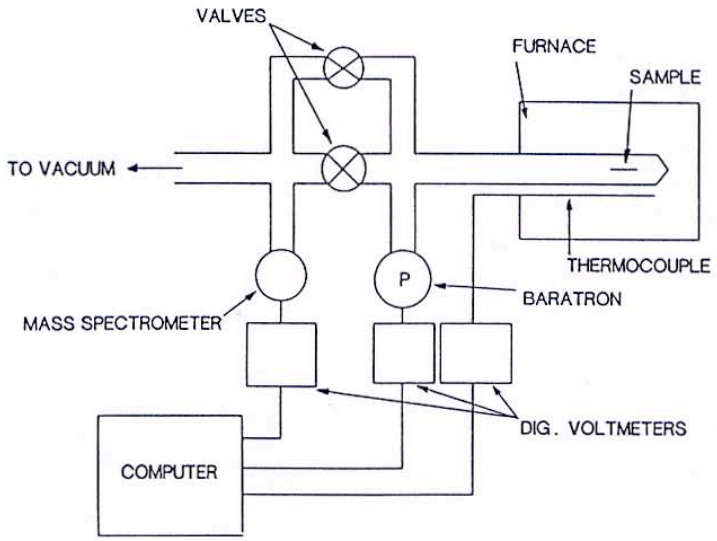

Fig. 1. Schematics of the gas evolution equipment : a sample is mounted in the quartz tube which is placed in a furnace. After the tube is pumped down and closed, the sample is heated and the pressure - due to gas evolution - is measured using a capacitance pressure gauge. The evolved gas is also analysed using a mass spectrometer.

A schematic drawing of the equipment is shown in Fig. 1. The sample ($\geq$ 0.1 mg) is mounted in an initially evacuated quartz tube (P $\simeq 10^{-6}$ Torr) and heated to $\simeq$ 1000°C, typically at a rate of 10°C/min. Due to evolution of gaseous elements out of the specimen, pressure builds up in the tube and can be monitored accurately using a capacitance pressure gauge (baratron) and a mass spectrometer. The resulting pressure versus temperature curve is corrected for the background signal arising from the empty tube (which never exceeds 5% of the total amount). Using the ideal gas law, the pressure can be related to the number x of oxygen atoms per unit cell which are escaping from the sample.

Typically, a pressure versus temperature (or x versus temperature) curve increases stepwise, since the gas evolution is a thermally activated process. By taking the temperature derivative, the steps are transformed into more clearly observable peaks. The area under a peak is proportional to x, while the peak temperature provides a good estimate for the activation energy (ΔG). Determination of x and ΔG can be done more rigorously by fitting the curve to a single site desorption relation

$$\frac{dx}{dT} = \mu(N - x)exp(-\frac{\Delta G}{k_B T}),$$

where μ is a frequency factor and N the initial oxygen content (7 - δ).

Figure 2 (a) shows the temperature derivative of x versus temperature for a sample with starting composition near $YBa_2Cu_3O_{6.9}$ ($T_c \simeq 92$ K). This result is reproducible and completely reversible : the original properties are recovered when the sample is cooled down slowly in an oxygen atmosphere. As already mentioned, the peaks showing up at different temperatures indicate the presence of several inequivalent oxygen sites in the material. This does not imply, however, that all these sites belong

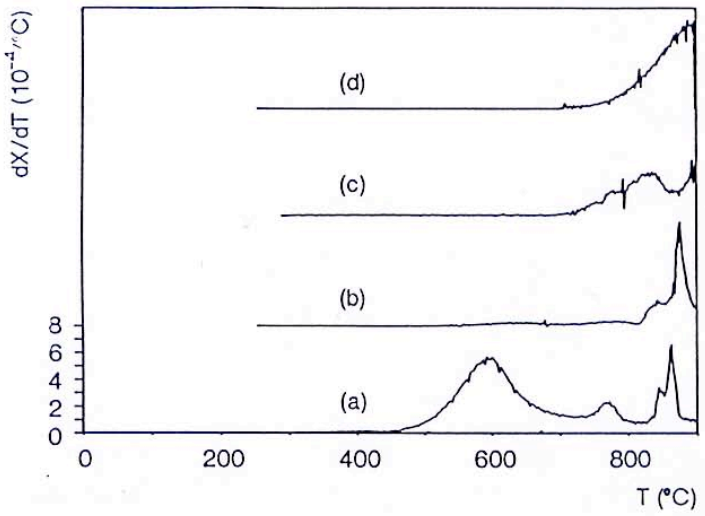

Fig. 2. Gas evolution spectra (temperature derivative of the number of evolved oxygen atoms versus temperature) for (a) $YBa_2Cu_3O_7$ compared to three impurity phases : (b)$BaCuO_2$, (c) Y_2BaCuO_5 and (d) $Y_2Cu_2O_5$.

to the stoichiometric 123 compound. The sample might contain small amounts of impurity phases which, in the case of amorphous phases, can not be detected by x-ray or neutron diffraction. Therefore, it is important to compare the YBCO evolution spectrum with spectra taken from impurity phases. In Fig. 2 we also show the evolution curves for (b) $BaCuO_2$, (c) Y_2BaCuO_5 and (d) $Y_2Cu_2O_5$. Looking at these curves, it becomes clear that the sharp peaks above 800°C in Fig. 2 (a) probably arises from impurities present in the sample. Indeed, the intensity of the high-temperature peaks depends on the details of the preparation and can be reduced substantially when adapting the preparation conditions. It is therefore very unlikely that these high-temperature peaks in the YBCO spectrum are caused by the stiochiometric 123 compound. Therefore, our main interest will be directed towards the oxygen evolution occuring at lower temperatures..

The low-temperature peak in Fig. 2 (a) (at $\simeq$ 600°C) can be fitted with x $\simeq$ 0.4 atoms per unit cell and $\Delta G \simeq 1.36$ eV, and has been assigned to oxygen atoms escaping from the Cu-O chains [5]. The latter assignment was made after comparing materials which are known to contain Cu-O chains ($YBa_2Cu_3O_7$, $LaBa_2Cu_3O_7$, $Y_{1-y}Pr_yBa_2Cu_3O_7$) with others not containing Cu-O chains (La_2CuO_4, $La_{2-y}Sr_yCuO_4$, Bi-Sr-Ca-Cu-O) (see Fig. 3). Only the samples with the chains exhibit the broad low- temperature peak. Moreover, this assignment is in agreement with earlier neutron scattering results [6].

The second peak (at $\simeq$ 720°C) which appears as a shoulder of the first one, probably arises from the same oxygen sites (O1/O5), and/or the O4 site in the Ba-O plane.

The above arguments show that the gas evolution technique is a very useful tool for sample characterization : it is able to determine the relative oxygen content, it can distinguish between oxygen atoms arising from different sites (e.g. Cu-O chains) and detects impurity phases which may even be amorphous.

An additional, important advantage of the gas evolution technique is the fact that very small samples can be studied. Higher accuracy is obtained when starting from a lower residual pressure and using a smaller quartz tube in conjunction with UHV techniques. In this way, quantitative statements can be made regarding oxygen content and kinetics in high T_c thin films.

2.2 High-Frequency Susceptometer

The correlation between the superconducting properties and the gas evolution has been studied by using a cryogenic tunnel diode High-Frequency (HF) oscillator. HF oscillators have been used extensively for measurements of various physical quantities [7] because of the great precision with which frequency changes can be measured. Measurements of the resonance frequency F of a LC oscillator can be used to detect extremely small changes in the inductance or capacitance of the circuit.

A scheme of the oscillator electronics is shown in Fig. 4. To avoid the parasitic inductance and capacitance of long transmission lines, the LC circuit as well as the HF oscillator are both put in the cryostat. Consequently, the choice of active and passive components is strongly limited. In our experiments, the oscillator is driven by a tunnel diode, which operates in the whole temperature range from 300 K down to 1.5 K. The sample to be measured is mounted in the coil L_o of the circuit. The DC power is supplied by two mercury batteries (2.7 V) kept at room temperature and is transmitted to the low-temperature electronics via the same coaxial cable used to pick up the HF signal for frequency detection. The tunnel diode provides a negative

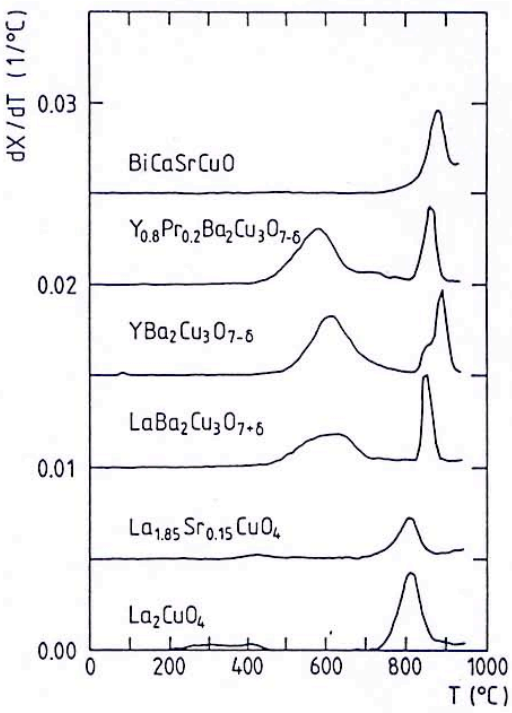

Fig. 3. Comparison between the evolution spectra for materials known to contain Cu-O chains and materials without these chains.

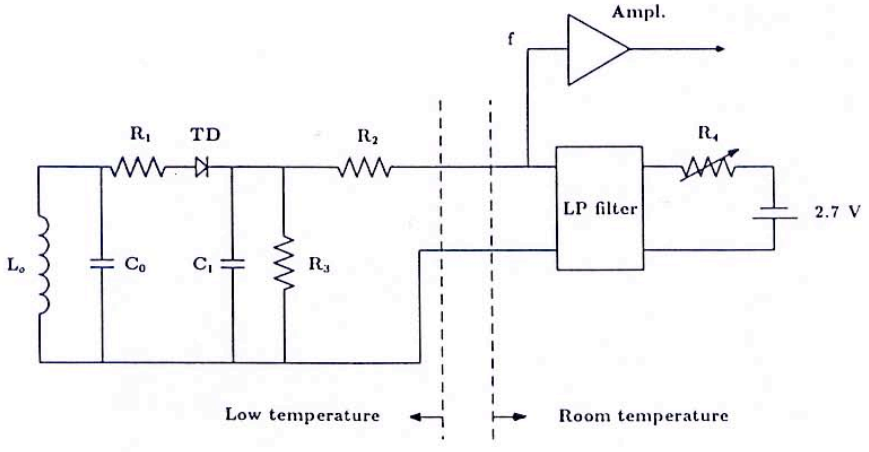

Fig. 4. Schematic view of the HF oscillator electronics. L_o = coil, R_1 = 7 Ω, R_2 = 240 Ω, R_3 = 10 Ω, C_1 = 22.2 pF, C_2 = 1000 pF, TD = Tunneldiode.

conductance to the L_oC_o circuit and therefore sustains the oscillation. R_1 suppresses the possible occurrence of higher frequencies; R_2, R_3 and R_4 provide the proper bias voltage for the tunnel diode.

By cooling this system from 300 K down to 10 K, the resonance frequency changes by less than 1 % . If a sample is mounted, a possible superconducting transition is signaled by a sharp step in the frequency versus temperature curve. The normalized (with respect to the sample mass) temperature derivative of this curve allows a precise determination of the onset, midpoint and completion of the superconducting transition. The area under the derivative curve is proportional to the Meissner fraction of the high T_c sample. Since the relative frequency change is proportional to the filling factor times the susceptibility of the sample [7], it is obvious that the sensitivity increases with the sample volume.

3 Experimental Results

3.1 Oxygen Deficient Bulk Samples

To study the effect of the oxygen concentration and ordering on the superconducting properties of YBCO, we have prepared oxygen deficient samples by annealing in vacuum ($P \simeq 10^{-6}$ Torr). Starting from samples made by the standard powder metallurgical techniques, we have applied long time (0 - 100 hrs) annealings at low temperature (400°C) to allow for proper oxygen ordering. Two kinds of experiments were performed. In a first experiment, a new sample of identical dimension was taken from the same batch for each annealing; in a second experiment the same sample was recycled several times. Both experiments gave similar results. The complete experiment consists of preparing the oxygen deficient sample (i.e. annealing at 400°C for long periods of time), measuring the HF susceptibility and resistivity as a function of temperature, and performing gas evolution from room temperature to 950°C in order to determine quantitatively the oxygen deficiency.

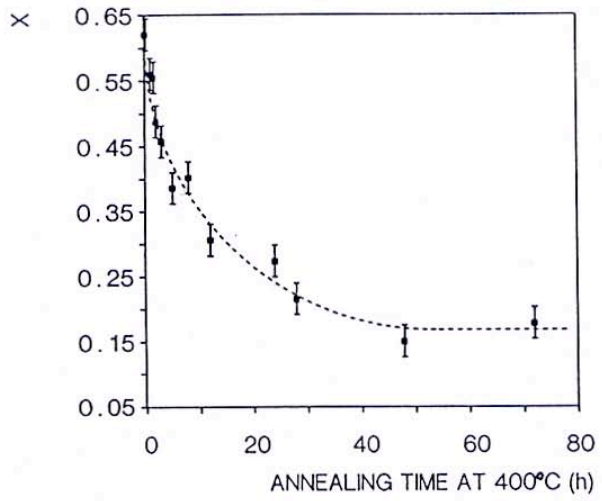

Fig. 5. Number of oxygen atoms per unit cell (x) escaping from the Cu-O chains in the evolution experiment, versus annealing time at 400°C in vacuum; the dotted line is drawn as a guide for the eye. (Absolute error on $x \simeq 0.05$)

When annealing, oxygen is lost from the Cu-O chains and therefore the intensity of the first peak in the evolution spectrum decreases as shown in Fig. 5, where the oxygen content under the first evolution peak is presented versus the annealing time at 400°C. A qualitative similar behavior is also observed for a repeated annealing of the same sample, i.e. a fast initial decrease of the oxygen loss with a consequent leveling off towards a constant value. The exact time after which the constant level is obtained, depends on sample size and density, as expected for solid-state diffusion.

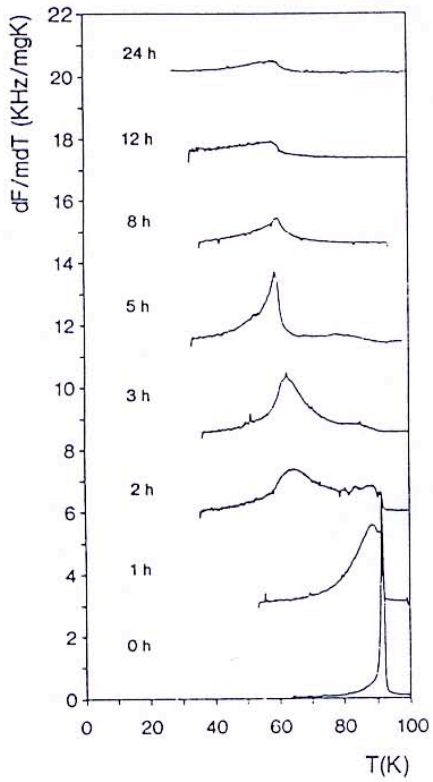

Fig. 6. Variation of T_c for samples with different annealing times. T_c is determined from the temperature derivative of the resonance frequency of the HF oscillator. The curves are shifted for clarity, and normalized with respect to the sample mass m.

Figure 6 shows a series of normalized critical temperature curves for various 400°C annealing times, obtained from HF susceptibility measurements. The curves for short ($\leq$ 1 hr) and long annealing times ($>$ 8 hrs) indicate the presence of one superconducting phase while for intermediate annealing times two clearly distinguishable superconducting phases are present. Each phase shows a similar behavior as a function of annealing time : a slow decrease of the peak temperature together with a broadening of the transition. Note that the high-temperature phase has the narrowest transition at 92 K (original sample), while the low temperature phase has the narrowest transition at $\sim$ 60 K after annealing for 5 hrs.

Defining the temperature where dF/dT is maximum (in Fig. 6) as T_c and the Full Width at Half Maximum (FWHM) of the peaks as the experimental error, it is possible to draw the variation of T_c as a function of annealing time (see Fig. 7). The T_c behavior shows a qualitative correlation with the oxygen evolution curves (Fig. 5). The decrease from 90 K towards 60 K can be explained by a decreasing oxygen

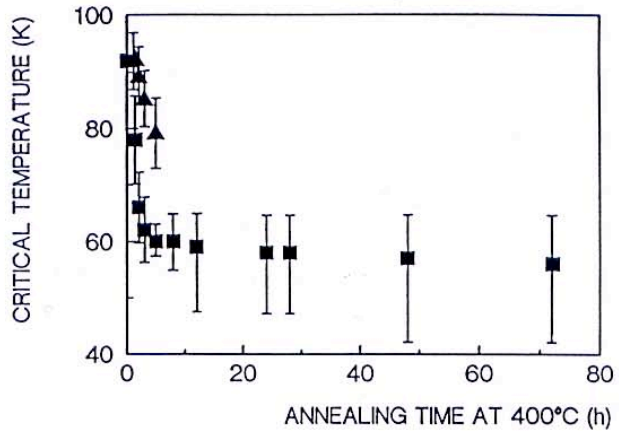

Fig. 7. Critical temperature (midpoint) versus annealing time. In the region where two phases coexist, the high T_c phase is presented by a triangle and the low T_c phase by a square. The error bars indicate the width of the transition (FWHM).

content (in the chains), in agreement with the picture in which the hole concentration determines the critical temperature. However, there is a second mechanism involved which tends to destroy the superconductivity. Indeed, on the T_c plateau (annealing times beyond 24 hours) the volume fraction of the low-temperature phase (integral under the dF/dT curve) decreases progressively for longer annealing times (Fig. 6) while the oxygen content stays constant. This behavior may be explained by a reorganisation of the remaining oxygen atoms : starting from an ordered configuration, the oxygen atoms might become disordered for longer annealing times. Much evidence has already been presented for the existence of oxygen ordering on the 60 K plateau ($0.3 < \delta < 0.5$) [8,9,10]. The most stable superstructure in this region of oxygen deficiency seems to be the orthorhombic II or $2a_o$ structure for which the a_o lattice parameter is doubled and which consists of filled (y = 0) and empty (y = 1) CuO_{1-y} chains. However, it remains still unclear whether this ordered phase is the 60 K superconducting phase or not. The order-disorder phenomena have still to be confirmed by detailed structural investigations using transmission electron microscopy and neutron diffraction.

The influence of the hole concentration on T_c has also been checked by substituting 20% , 40% and 60% of Y with Pr in $YBa_2Cu_3O_{7-\delta}$. The critical temperature shown in Fig. 8 drops from 90 K to 75 K (curve (a)), 55 K (curve (b)) and 0 K (curve (c)) respectively, for the three concentrations of Pr, in agreement with other experiments [11,12,13]. Gas evolution experiments were also performed on these compounds, yielding no difference at all in oxygen content (Fig. 9 (a) 20%, (b) 40%, (c) 60% Pr).

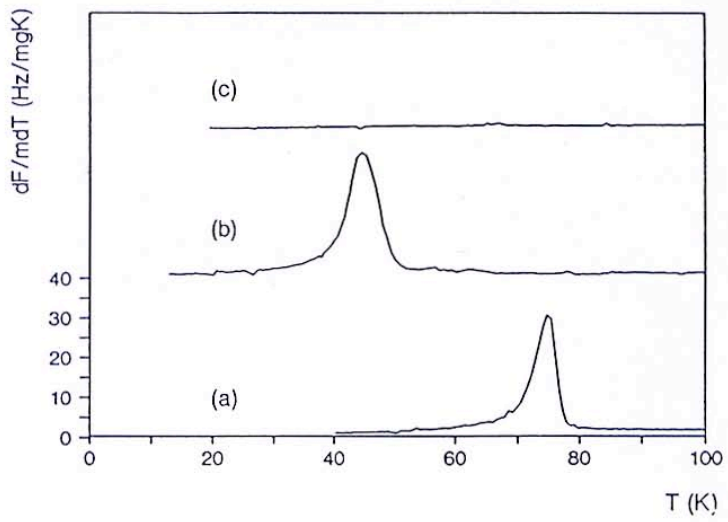

Fig. 8. Critical temperature for three different amounts of Pr substitution in $YBa_2Cu_3O_{7-\delta}$: (a) 20%, (b) 40% and (c) 60% Pr substituted for Y. Curves are shifted for clarity and normalized with respect to the sample mass m.

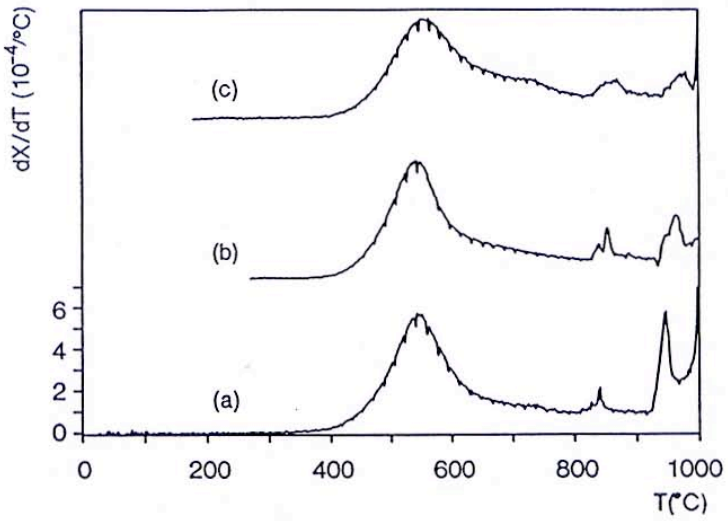

Fig. 9. Evolution spectra for three different amounts of Pr substitution in $YBa_2Cu_3O_{7-\delta}$: (a) 20%, (b) 40% and (c) 60% Pr substituted for Y. Curves are shifted for clarity.

This means that no extra change in hole concentration must be taken into account due to an extra oxygen loss or uptake, and the variations in T_c are solely due to the Pr substitution. The reason for these changes is not obvious. Spectroscopic measurements by a number of groups (see for instance ref. [14]) have claimed that Pr is invariably in an oxidation state of 3+ and therefore no changes should occur

in the hole concentration. However, it should be pointed out that all spectroscopic measurements are only sensitive to the surface (< 100 Å) and therefore it is not clear how to assign a formal oxidation state for Pr in the bulk. An alternative, quite attractive idea is to assume an oxidation state higher than 3+ for Pr, as occurs in many of its oxides. If this is true, the changes in T_c with Pr substitution, can be explained by a change of the hole density in the CuO_2 planes [11,12,13,15].

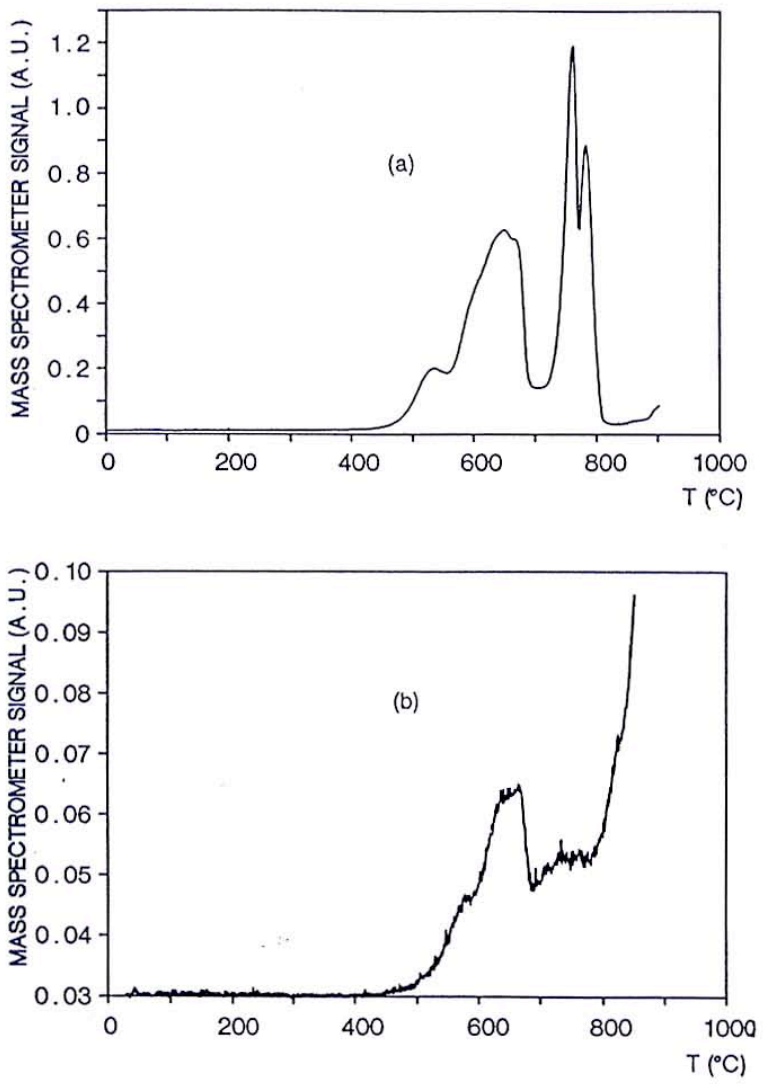

Fig. 10. Temperature dependence of the oxygen evolution measured using a quadrupole mass spectrometer : (a) for a superconducting and (b) a non-superconducting YBCO thin film.

3.2 Thin Films

Finally, we present preliminary gas evolution results obtained for YBCO thin films. Two films were investigated : a superconducting film prepared by MBE on MgO [16] with a $T_c \simeq 78$ K, and a non- superconducting film prepared by laser ablation on Al_2O_3. In both cases, the evolution of oxygen was studied by monitoring the gas with the mass spectrometer tuned at fixed mass number (i.e. 32 for O_2). The results are shown in Fig. 10. Curve (a) was taken for the non-superconducting film, while (b) is for the superconducting film. The low-temperature shape of both curves is very similar, but the signal is one order of magnitude stronger in the superconducting film (b), while both films (thickness ~ 1 μm) have the same mass. The high-temperature part is quite different, indicating the presence of different impurity phases. These preliminary results indicate that the oxygen kinetics in thin films seems to be very similar to bulk material, with the films yielding even more fine structure in the low-temperature "chain" part.

4 Conclusion

We have shown that for long annealing times at 400°C, two distinct superconducting phases develop. The transition temperature decreases and the transition width broadens with increasing annealing time. The sharpest transition occurs for $T_c \approx 90$ K and $T_c \approx 60$ K. In addition, the volume fraction of the 60 K phase decreases with increasing annealing times although the oxygen concentration remains fixed. Substitution with Pr on the Y site can be accomplished without changes in the oxygen stoichiometry and with an important depression of the superconducting transition temperature. All these studies indicate that the superconductivity in YBCO is determined by two mechanisms : the hole concentration and the oxygen ordering. Further structural investigations are underway to address these issues.

Acknowledgements

We thank Dr. C. Deneffe for providing us with some laser ablation thin films. This work is supported by the Belgian F.K.F.O., the I.U.A.P. and G.O.A. Programs (at K.U.L.) and the U.S. National Science Foundation under grant No. 8803185 (at U.C.S.D.). International travel was provided by a NATO grant. B.W. is a Research Fellow of the Belgian F.K.F.O., J.V. is a Research Fellow of the Belgian I.W.O.N.L., and C.V.H. is a Research Associate of the Belgian N.F.W.O.

References

[1] Y. Bruynseraede, J. Vanacken, B. Wuyts, C. Van Haesendonck, J.-P. Locquet and Ivan K. Schuller, to be published in Physica Scripta.

[2] R.J. Cava, B. Batlogg, C.H. Chen, E.A. Rietman, S.M. Zahurak and D.J. Werder, Nature, **329**, 423 (1987); ibidem, Phys. Rev. B **36**, 5719 (1987).

[3] Y. Song, J.P. Golben, X.D. Chen and J.R. Gaines, Phys. Rev. B **38**, 2858 (1988).

[4] J.P. Locquet, H. Strauven, B. Wuyts, O.B. Verbeke, K. Zhang, I.K. Schuller, J.

Vanacken, C. Van Haesendonck and Y. Bruynseraede, Physica C **153-155**, 822 (1988).

[5] J.-P. Locquet, J. Vanacken, B. Wuyts, Y. Bruynseraede, K. Zhang and Ivan K. Schuller, Europhys. Lett. **7**, 469 (1988).

[6] J.D. Jorgensen, M.A. Beno, D.G. Hinks, L. Soderholm, K.J. Volin, R.L. Hitterman, J.D. Grace, Ivan K. Schuller, C.U. Segre, K. Zhang and M.S. Kleefisch, Phys. Rev. B **36**, 3608 (1987); J.D. Jorgensen, H. Shaked, D.G. Hinks, B. Dabrowski, B.W. Veal, A.P. Paulikas, L.J. Nowicki, G.W. Crabtree, W.K. Kwok and L.H. Nunez, Physica C **153-155**, 578 (1988).

[7] B. Van Riet and L. Van Gerven, J. Phys. E : Sci. Instrum. **15**, 558 (1982).

[8] D.J. Werder, C.H. Chen, R.J. Cava and B. Batlogg, Phys. Rev. B **37**, 2317 (1988); Phys. Rev. B **38**, 5130 (1988).

[9] J. Reyes-Gasga, T. Krekels, G. Van Tendeloo, J. Van Landuyt, S. Amelinckx, W.H.M. Bruggink and H. Verweij, Physica C **159**, 831 (1989).

[10] Y. Kubo, T. Ichihashi, T. Manako, K. Baba, J. Tabuchi and H. Igarashi, Phys. Rev. B **37**, 7858 (1988).

[11] Y. Dalichaouch, M.S. Torikachvili, E.A. Early, B.W. Lee, C.L. Seaman, K.N. Yang, H. Zhou and M.B. Maple, Solid State Commun. **65**, 1001 (1988).

[12] L. Soderholm, K. Zhang, D.G. Hinks, M.A. Beno, J.D. Jorgensen, C.U. Segre and I.K. Schuller, Nature **328**, 604 (1987).

[13] B. Okai, M. Kosuge, H. Nozaki, K. Takahashi, M. Ohta, Jpn. J. Appl. Phys. **27**, L41 (1988).

[14] P. Sladeczek, U. Neukirch, C.T. Simmons, O. Strebel, C. Laubschat, D.D. Sarma and G. Kaindl, Physica C **153-155** 916 (1988).

[15] M.E. Lopez-Morales, D. Rios-Jara, J. Taguena-Martinez and R. Escudero, Physica C **153-155**, 942 (1988).

[16] K.Y. Yang, H. Homma, R. Lee, R. Bhadra, J.-P. Locquet, Y. Bruynseraede and Ivan K. Schuller, Proc. MRS Spring Meeting, EA-14, 357 (1988).